

MULTIZONAL INTEGRAL PROPORTIONAL SPEED CONTROLLER FOR A DC MOTOR FED BY SEPIC CONVERTER

N. T. Tweig

Academy of Specialist Studies, Workers University, Egypt

ABSTRACT

This paper presents a multizonal integral proportional (IP) speed controller for a closed loop speed controller of a separately excited dc motor. The motor is fed from a dc power supply and sepic converter. This converter offers both step-up and step-down characteristics of the motor terminal voltage. A high performance is achieved with a simple control circuit having only one switch (MOSFET) for the proposed system. The output voltage and current are smooth and free of ripples. The converter operates in both open and closed loop speed control. A multizonal IP speed controller is used to overcome the possibility of change in the system parameters. The proposed modeling and simulation of the system are performed using differential equations which describe the system behaviour in the different operating conditions. The run up, transient and steady state are presented. Speed control using multizonal IP speed controller is given to satisfy the best required response for the load disturbances. Also, the motor speed can follow the desired reference speed smoothly in the different operating zones. The experimental results have ensured the proposed controller robustness, simple, and powerful control application capabilities. The experimental and simulation results of the converter for both open and closed loop speed control system are verified and a good correlation between them was found.

يقدم البحث محكم سرعة متعدد المناطق تكاملي تناسبى وذلك للتحكم في السرعة للمسار المغلق لمحرك تيار مستمر ذو إثارة منفصلة. تتم تغذية المحرك من منبع جهد مستمر ومحوال من نوع SEPIC. يقدم هذا المحوال خواص الرفع والخفض على جهد أطراف المحرك. أمكن الحصول على خواص عالية لهذا النظام المقترح باستخدام دائرة تحكم بسيطة ذات مفتاح واحد للمحوال من نوع الموسفت، حيث تم الحصول على جهد وتيار الخرج ذو شكل منتظم وخالى من التذبذبات. يعمل المحوال في حالتي التحكم في السرعة للدائرتين المفتوحة والمغلقة. كما تم استخدام محكم للسرعة متعدد المناطق وذلك للتغلب على حالات التغير في ثوابت النظام. تم اقتراح نموذج للنظام وتمثيله باستخدام المعادلات التفاضلية التي تصف خواص النظام لحالات التشغيل المختلفة مثل الحالات العابرة وحالة الاستقرار. تم اقتراح نظاما للتحكم في السرعة باستخدام محكم سرعة تكاملي تناسبى متعدد المناطق وذلك للحصول على أفضل استجابة مطلوبة لحالات حدوث تغير في الأحمال وفي سرعة الاسناد. تم الحصول على النتائج العملية للتأكد من أن المحكم المقترح قوى ومتميز وبسيط وذو قدرة كبيرة على تطبيقات التحكم المختلفة. تمت المقارنة بين النتائج العملية والنظرية لنظامي التحكم في السرعة لحالتي الدائرة المفتوحة والمغلقة، وقد وجد أن هناك تطابقا كبيرا بين الحالتين.

Keywords: Sepic converter, Multizonal integral proportional controller, Separately excited DC motor, Speed control, DC to DC converter.

1. INTRODUCTION

Direct current motor drives are used extensively in industries such as steel mill, paper mill, conveyors, and chemical industries. In many drive applications, the mechanical load varies considerably during operation. Such examples of this load are robots and machine tools. When a fixed controller setting is used for a dc drive system with wide load changes, unsatisfactory performance is often produced [1].

High performance dc motor drives are important for multitude of industrial applications [2]. Precise, fast, effective speed reference tracking with minimum overshoot/undershoot and small steady state error are essential control objectives. Conventional controllers are usually used for fixed structure, and fixed parameters design [3-5]. Tuning and optimization of these controllers are challenging and have difficult task, particularly under varying load conditions, and abnormal operation.

An artificial intelligent system based on fuzzy logic and neural network techniques was reported for a high performance dc drive [6]. A simulation study for an intelligent rule-based error driven gain scheduling controller for a chopper fed dc series motor was proposed in [7]. Alternatively, an intelligent self-adaptive rule based speed regulator for a permanent magnet dc motor drive is implemented in [8]. The dynamic and steady state performance of a symmetrical angle controlled dc motor is investigated, and the power factor of the system is improved using this technique. Also, the conventional analog proportional integral controller is used for speed control [9].

It is well known that power supplies can suffer considerably from current distortions and low power factor operations when a conventional diode bridge rectifier is operated with a dc filter capacitor at the output terminal. They result in large installation size and increased losses. To counteract these shortcomings, various passive and active input current wave shaping methods have been presented [10-13]. The supply currents can be passively wavelshaped by connecting the series resonant circuit or parallel resonant circuit [10] with the supplies in series. However, it is difficult to obtain sinusoidal supply currents with a near unity power factor for a wide variety of operating conditions. On the other hand, when the cascade combinations of a diode bridge and boost dc-dc converter are used as the rectifiers, the sinusoidal supply currents can then be actively wavelshaped with a near unity power factor operation by filtering the high order current harmonics if the rectifiers are operated in discontinuous current conduction mode [11-17]. They also have the advantage of simple pulse width modulation (PWM) with uniform duty factor and a single power switching device which provides the necessary control over the currents both in single phase [11-12] and three phase [13] configurations. Unfortunately, if both step-up and step-down output voltages, which have to be continuously regulated, are desired, they cannot satisfy the requirement. If, for example, the rectifier inverter system is considered, the rectifier with step-up and step-down characteristics will be useful because it enables the system to operate with pulse amplitude modulation at the inverter input terminal. Thus, PWM techniques for the inverter circuit may be merely focused on the decreasing in output ac voltage harmonics.

In the previous researches, they haven't paid an attention for the dynamic operation of a dc to dc sepic converter fed dc motor. Also, they haven't paid an attention for some different points of the operation with the load and speed reference changes. They have focused on one operating point only with IP speed controller.

In this paper, a speed control for a separately excited dc motor fed from dc supply through a sepic converter is presented. Step-up and step-down characteristics of the output voltage are obtained. A multizonal integral proportional speed controller is applied. The proposed modeling and numerical simulation of the investigated system is described in different modes of operation. An experimental system is built to verify the simulation results. The comparison between the experimental and simulation results has proved a good agreement with each other. Both results give a prediction with a high motor speed performance over a wide range of reference speed and load changes.

2. SYSTEM DESCRIPTION

Figure (1) shows the schematic diagram of the proposed system. The capacitor C_1 acts as a transfer element. The inductance L_2 and capacitance C_2 are used as a filter to obtain dc output load voltage with minimum ripples. The switching frequency (F_s) and the value of C_1 are determined according to L_1 value. The resonance frequency is calculated from the equation $f_r = \frac{1}{2\pi\sqrt{L_1C_1}}$ and should be

sufficiently higher than the switching frequency to prevent any resonance phenomenon in the ac circuit. The system parameters are given in the Appendix.

Step-up and down behaviour of the output voltage is obtained by regulating the control voltage (V_c) from zero to the maximum value of the carrier voltage (V_{car}). The Mosfet is derived on when the carrier voltage (V_{car}) is lesser than or equal to the control voltage, which is the speed control output. The duty ratio is given :

$$\text{Duty ratio} = \frac{T_{on}}{T_{on} + T_{off}} \quad (1)$$

Where T_{on} = the Mosfet on time.

T_{off} = the Mosfet off time.

3. SYSTEM MODELING AND SIMULATION

To simulate the detailed operation, the voltage, current and motor equations have to be established for each operating mode.

Mode (1):

In this mode the Mosfet is on and the current i_1 will flow in the loop ($v - L_1 - r_1$). The capacitor C_1 will discharge where the diode D is off. The equations describing this mode are:

$$\frac{di_1}{dt} = \frac{v - r_1 i_1}{L_1} \quad (2)$$

where v is the dc input voltage

$$\frac{dv_{c1}}{dt} = \frac{-i_2}{C_1} \quad (3)$$

where i_1 and i_2 are the currents of coils 1 and 2 respectively, r_1 and r_2 are the internal resistance of coils 1 and 2 respectively.

$$\frac{di_m}{dt} = \frac{v_m - r_m i_m - k_m \omega_m}{L_m} \quad (4)$$

$$\frac{d\omega_m}{dt} = \frac{k_m i_m - B\omega_m - T_1}{J} \quad (5)$$

Where, v_m , i_m , ω_m are the motor voltage, current and speed respectively. r_m and L_m are the motor armature resistance and inductance respectively. k_m is the motor back emf constant.

$$\frac{dv_m}{dt} = \frac{-i_m}{C_2} \quad (6)$$

where C_2 is the output filter capacitance.

Mode (2):

In this mode the Mosfet is off and the diode D is on. The current i_1 is greater than zero (i.e. positive). The corresponding differential equations describing this mode are :

$$\frac{di_1}{dt} = \frac{v - r_1 i_1 - v_{c1}}{L_1} \quad (7)$$

$$\frac{dv_{c1}}{dt} = \frac{i_1}{C_1} \quad (8)$$

$$\frac{di_m}{dt} = \frac{v_m - r_m i_m - k_m \omega_m}{L_m} \quad (9)$$

$$\frac{d\omega_m}{dt} = \frac{k_m i_m - B\omega_m - T_1}{J} \quad (10)$$

$$\frac{dv_m}{dt} = \frac{i_2 - i_m}{C_2} \quad (11)$$

$$\frac{di_2}{dt} = \frac{-r_2 i_2 - v_m}{L_2} \quad (12)$$

Mode (3):

In this mode, the Mosfet is off, diode D is on and the current i_1 is equal to zero. The corresponding differential equations which describe this mode are:

$$\frac{di_m}{dt} = \frac{v - r_m i_m - k_m \omega_m}{L_m} \quad (13)$$

$$\frac{d\omega_m}{dt} = \frac{k_m i_m - B\omega_m - T_1}{J} \quad (14)$$

$$\frac{dv_m}{dt} = \frac{i_2 - i_m}{C_2} \quad (15)$$

$$\frac{di_2}{dt} = \frac{-r_2 i_2 - v_m}{L_2} \quad (16)$$

Mode (4):

In this mode the Mosfet is off and the diode D is off also. The both currents i_1, i_2 are equal to zero. The corresponding differential equations describing this mode are :

$$\frac{di_m}{dt} = \frac{v_m - r_m i_m - k_m \omega_m}{L_m} \quad (17)$$

$$\frac{d\omega_m}{dt} = \frac{k_m i_m - B\omega_m - T_1}{J} \quad (18)$$

$$\frac{dv_m}{dt} = \frac{-i_m}{C_2} \quad (19)$$

4. SIMULATION AND EXPERIMENTAL RESULTS

4.1 Steady-State Performance Results

The relation between the duty ratio and the motor speed is shown in Figure (2) at different ratios from the full load. It is noticed that the speed is increased with the increasing of the control voltage. Figure (3) shows the relation between the duty ratio and the motor current. It is observed that the motor current value is constant with the increasing of the duty ratio. That is because the load torque value is constant during every ratio of the full load. Figure (4) and (5) clarify the relation between the duty ratio and motor voltage and supply current respectively. It is noticed that both the motor voltage and supply current increase with the increasing of the duty ratio.

4.2 Steady-State waveforms Results

This study is made at half full load torque (0.065 N.m) with a constant value of control voltage (duty ratio) equals 0.35. The figures show the simulation and experimental results for different parameters. Figure (6) shows the motor current versus time during the steady state condition. It is observed that the motor current remains constant with time, since the load torque is constant Figure (7) shows the variation of the coil current with time, while Figure (8) shows the variation of the source current under the same condition of operation. The motor voltage

versus time is as shown in Figure (9). As for the source voltage, it is as shown in Figure (10). Also, both the simulation and experimental results clarify that the motor voltage and source voltage remain constant with time.

4.3 Starting up Performance Results

The results are taken and simulated for the same parameters under the starting up condition, and in case of the half load and constant control voltage of 0.35. Figure (11) shows the variation of the motor current versus time. Figure (12) shows the motor speed under the same conditions. Figure (13) shows the variation of the source current versus time, while Figure (14) shows the variation of the motor voltage with time. As for the source voltage, Figure (15) shows that it remained constant with time in the starting up behaviour.

4.4 Transient Performance Results

Two kinds of changes have been proposed in order to study the characteristics of the system. The first change is a step change in the control voltage. The load is taken constant at the value of half full load. A positive step change from 0.25 to 0.35 volt in the control voltage is taken. Figure (16) shows the simulation and experimental result for the motor speed against time. Figures (17),(18) show the same previous parameters due to a negative step change in the control voltage from 0.35 to 0.25 volt.

The second change is in the load. A positive change in load is taken from a light load to the full load. The simulation and experimental results are given for the main system parameters. The motor current versus time is shown in Figure (19). The motor speed is as shown in Figure (20). The motor voltage versus time is shown in Figure (21). The same previous parameters due to a negative change in the load are studied. Figure (22) shows the change in the motor current. The motor speed versus time is shown in Figure (23). Figure (24) shows the motor voltage versus time due to the negative change in the load.

5. CLOSED LOOP SPEED CONTROL

5.1 The System Transfer Function

The open loop transfer function of the speed response with a step change in the control voltage for all the system is obtained and is given as

$$T.F = \frac{K_S}{1+T_{em}S} \quad (20)$$

Where, $K_S = 11.5$ and $T_{em} = 0.09$ sec.

Figure (25) shows the complete block diagram for the closed loop system. A multizonal speed controller is designed to obtain a wide range of the speed

control using different integral proportional (IP) controllers for different operating points. The load is divided into three zones. Zone one is from 0.25 to 0.5 of the full load. Zone two is from 0.5 to 0.75 of the full load. Zone three is from 0.75 to the full load. For any load zone the IP speed controller is designed.

5.2 Design of the IP Speed Controller

The open loop transfer function of the system is obtained according to Figure (25) as follows:

$$\frac{\omega_m(S)}{V_{ref}(S)} = \left(\frac{K_1 K_S K_t}{\tau_1 S}\right) \left(\frac{1}{1+T_{em}S}\right) \quad (21)$$

In order that the system becomes stable, the cross over frequency (ω_{CO}) for a phase margin more than 45° is found from the equation [18] :

$$\omega_{CO} = \frac{K_1 K_S K_t}{\tau_1} \quad (22)$$

The parameters of the speed controller for the three zones are given in the Appendix.

5.3 Controller Equations

The controller equations are given as:

$$\tau_1 \left(\frac{dO}{dt}\right) = V_{ref} - K_t \omega_m \quad (23)$$

$$V_C = K_1 (O - K_t \omega_m) \quad (24)$$

5.4 Closed Loop Simulation and Experimental Results

Zone two is taken as an example. Figure (26) shows the experimental and simulation result for the motor speed due to a positive load change from 0.5 to 0.75 from the full load, while Figure (27) shows the same result but for a negative load change from 0.75 to 0.5 from the full load. It is noticed that the speed is changed and then returned to its initial value. Figure (28) shows the simulation and experimental results for a positive step change in V_{ref} from 1100 to 1750 r.p.m., while Figure (29) shows the results for a negative step change from 1750 to 1100 r.p.m. It is observed that the speed can follow the desired reference speed smoothly.

6. CONCLUSIONS

The paper presents the modeling, simulation and experimental behaviour for dynamic and steady state performance of a separately excited dc motor fed from a sepic dc to dc converter. The use of a sepic converter achieved the availability to obtaining the step-up and step-down characteristics of the motor input voltage. The presented control circuit for this system is simple since only one switch is used. The obtained dc motor voltage and current has the

advantage to be approximately free of ripples. The dynamic and steady state behaviour are obtained using the proposed modeling and numerical simulation. The suitable parameters in designing the integral proportional speed controller are obtained for three zones of load in order to obtain a constant speed when there is a wide range of load change. Also, it is found that the motor speed can follow the desired reference speed smoothly. The comparison between the simulation and experimental results for open and closed loop for the speed control has proved that they are in an agreement with each other.

7. REFERENCES

- [1] M.A.El-Shorkawi, and S.Weerasooriya, "Development and Implementation of Self Tuning Tracking Controller For D.C Motors" IEEE Trans. On Energy Conversion, Vol. 5, March 1990, pp. 122-128.
- [2] S.Weerasooriya, and M.A.El-horkawi, "Adaptive Traction Control For High Performance DC Drives" IEEE Trans. On Energy Conversion, Vol. 4, No. 3, September 1989, pp. 502-508.
- [3] B.A.White, et al, "A Simple Digital Control Scheme For DC Motor", IEE Proc. B, Vol. 130, March 1992, pp. 143-147.
- [4] A.J.Dymock, "Analysis Of A Type Of Model Reference Adaptive Control System" IEE Proc. Vol. 112, March 1965, pp. 743-753.
- [5] E.H.Mandani, "Application Of Fuzzy Logic To Approximate Reasoning Using Linguistic Synthesis" IEEE Trans. On Computer, Vol. C-26, No. 12, December 1977, pp. 1182-1191.
- [6] S.Weerasooriya, and M.A.El-horkawi, "Identification and Control of a DC Motor Using Back Propagation Neural Networks" IEEE Trans. On Energy Conversion, Vol. 6, No. 4, December 1991, pp. 1538-1541.
- [7] H.F.Soliman et al, "Intelligent Rule Based Error Driven Gain Scheduling Controller For Chopper Fed DC Series Motor" Al-Azhar Engineering Fourth International Conference, 16-19 December 1995.
- [8] A. S. Abdel-Ghaffar, S. S. Shokralla and A. M. Sharaf, "An Intelligent Self Adaptive Rule Based Regulator for Permanent Magnet DC Motor drive" Proc. of Cairo IASTED International Conference Computer Application in Industry, Ain Shams University, 26-29 December 1994.
- [9] S. S. Shokralla and M. E. El-Shibiny, "Dynamic and Steady State Performance of a Symmetrical Angle Controlled DC Motor" Engineering Research Bulletin, ISSN, 1110-1180, Vol. 23, No. 2, 2000, pp. 211-230.
- [10] A. R. Prasad, P. D. Zigas and S. Manias, "Passive Input Current Wave shaping Method For Three Phase Diode Rectifiers", IEE Proc. B, 1992, 139, (6), pp.512-520.
- [11] K. H. Liu and Y. L. Lin, "Current Wave Form Distortion in Power Factor Correction Circuits Employing Discontinuous Mode Boost Converters", IEEE PESC, 1980, pp. 825-829.
- [12] T. C. Chen and C. T. Pan, "Modeling and Design of a Single Phase AC to DC Converter", IEE Proc. B, 1992, 139, (5), pp.465-470.
- [13] A.R.Prasad, P.D.Zigas and S.Manias," An Active Power Factor Correction Technique For Three Phase Diode Rectifiers" IEEE Trans. PE-6,(1) 1991, pp. 83-92.
- [14] H. Oishi et al, "Sepic Derived Three Phase Sinusoidal Rectifier Operating in Discontinuous Current Conduction Mode" IEE Power Application, Vol.142, No. 4, July 1995, pp. 239-245
- [15] D. S. L.Simonetti et al, "The Discontinuous Conduction Mode Sepic and Cuk Power Factor Pre-regulators: Analysis and Design", IEEE Trans. On Industrial Electronics, Vol. 44, No. 5, 1977, pp. 630-637.
- [16] M. M. R. Ahmed, G. A. Putrus and S. S. Shokralla, "A New Approach for Speed Control of a DC Motor Fed From AC to DC Sepic Converter" 18th International Conference On Electricity Distribution, Turin, 6-9 June, 2005.
- [17] D. S. L. Simonetti et al, " Design Criteria for Sepic and Cuk Converters as Power Factor in Discontinuous Conduction Mode", Proc. of IECON' 92, pp. 283-288.
- [18] S. S. Shokralla, " A Simplified Approach for Closed Loop Speed Control of a DC Motor Using AC to DC Converter", Alexandria Engineering Journal, Vol. 36, NO. 2, March 1997.

8. APPENDIX

The parameters of the designed system are:

The test motor is a separately excited dc motor, 55 volt, 50 watt, 1 ampere, 3000 r.p.m. having the following measured parameters:

$r_m = 10.5 \Omega$, $L_m = 0.06 \text{ H}$, $r_f = 550 \Omega$,
 $J = 0.00015 \text{ kg.m}^2$, $k_m = 0.127 \text{ Volt}/(\text{rad./sec.})$,
 $B = 0.0001 \text{ Nm}/(\text{rad./sec.})$

The SEPIC converter parameters are:

$r_1 = 1.5 \Omega$, $L_1 = 0.025 \text{ H}$, $r_2 = 1.5 \Omega$,
 $L_2 = 0.048 \text{ H}$, $C_1 = 29 \mu\text{F}$, $C_2 = 1200 \mu\text{F}$,
 $V = 40 \text{ volt}$, $F_s = 2 \text{ kHz}$

The values of the integral proportional Controller parameters for the three zones are:

Zone (1) $K_1 = 0.9$, $\tau_1 = 0.09$
 Zone (2) $K_1 = 0.8$, $\tau_1 = 0.12$
 Zone (3) $K_1 = 0.7$, $\tau_1 = 0.18$

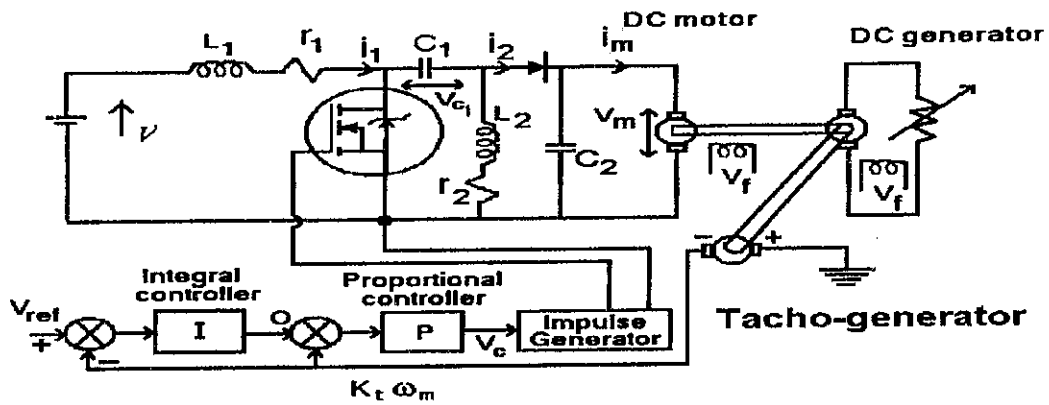


Fig. 1 Schematic diagram of the proposed system

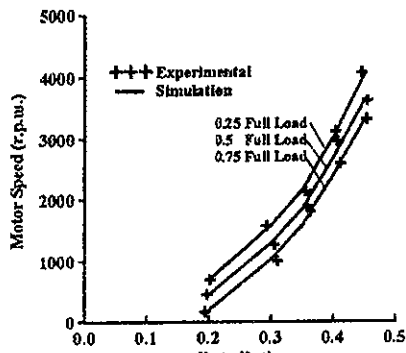


Figure (2) Motor Speed Versus The Duty Ratio During The Steady State Condition

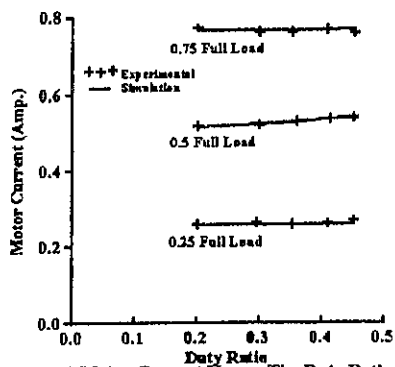


Figure (3) Motor Current Versus The Duty Ratio During The Steady State Condition

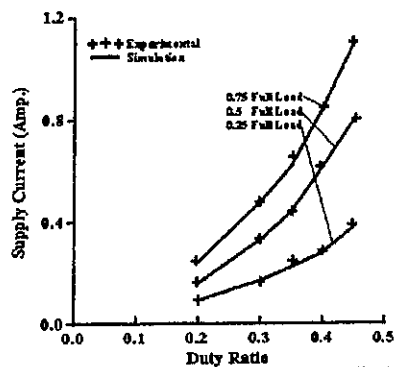
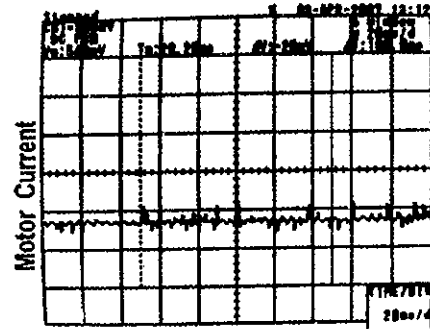


Figure (5) Supply Current Versus The Duty Ratio During The Steady State Condition



(a) Experimental Result

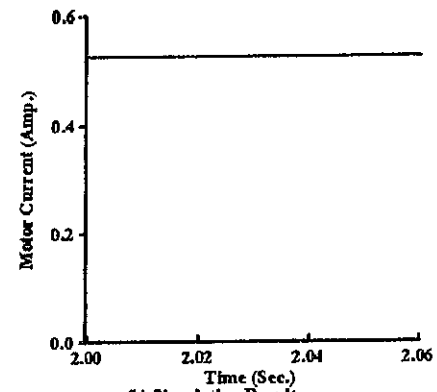
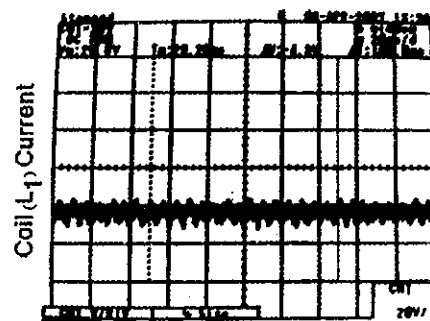


Figure (6) Motor Current Versus Time Due to Steady State Condition



(a) Experimental Result

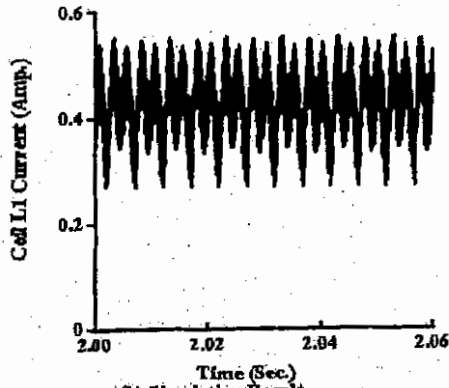
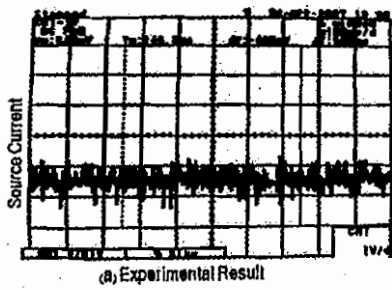


Figure (7) Coil Current Versus Time Due to Steady State Condition



(a) Experimental Result

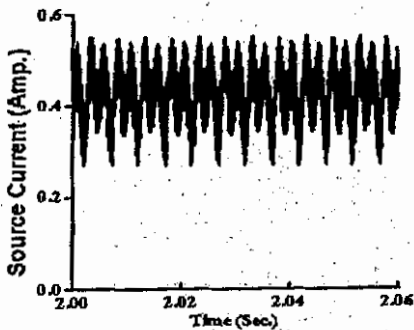
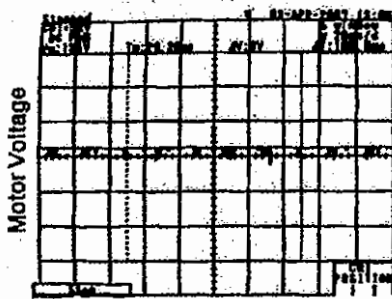


Figure (8) Source Current Versus Time Due to Steady State Condition



(a) Experimental Result

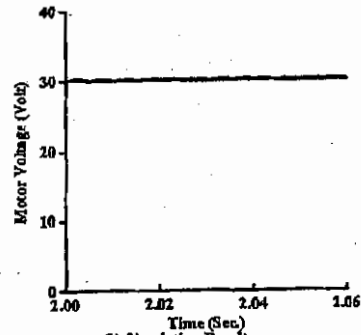
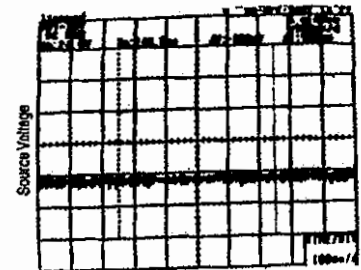


Figure (9) Motor Voltage Versus Time Due to Steady State Condition



(a) Experimental Result

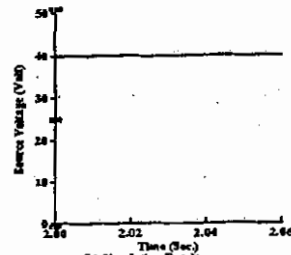
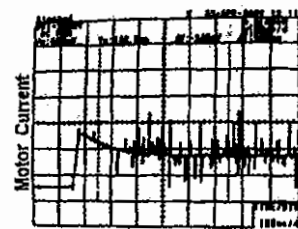


Figure (10) Source Voltage Versus Time Due to Steady State Condition



(a) Experimental Result

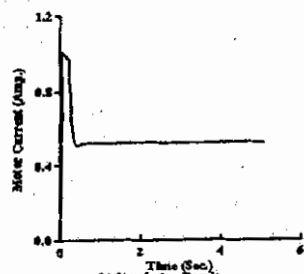


Figure (11) Motor Current Versus Time Due to Starting Condition

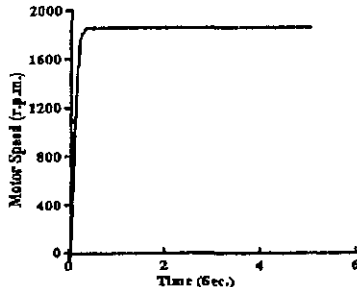
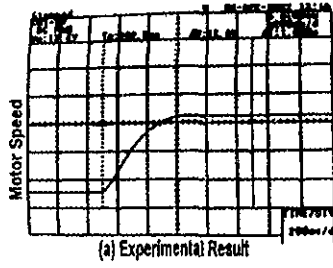


Figure (12) Motor Speed Versus Time Due to Starting Condition

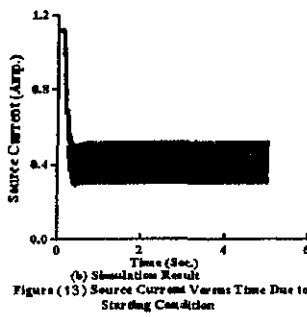
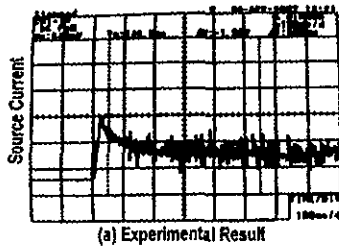


Figure (13) Source Current Versus Time Due to Starting Condition

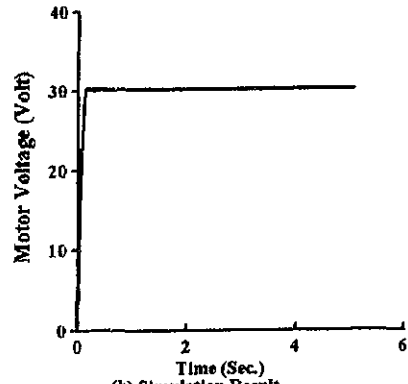
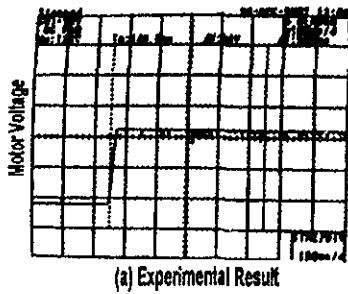


Figure (14) Motor Voltage Versus Time Due to Starting Condition

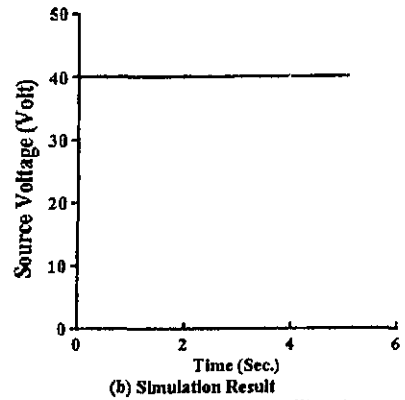
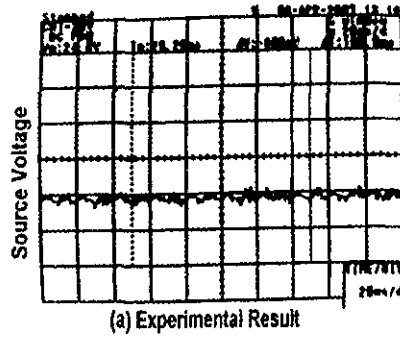
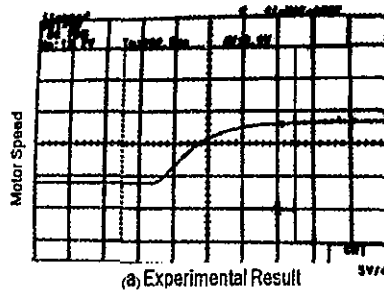
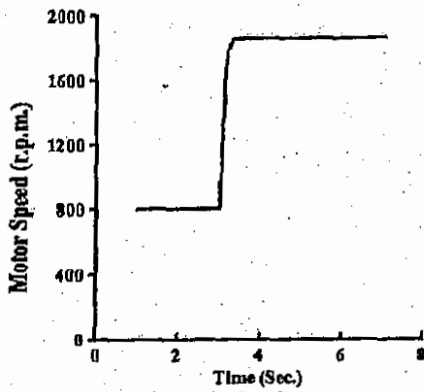
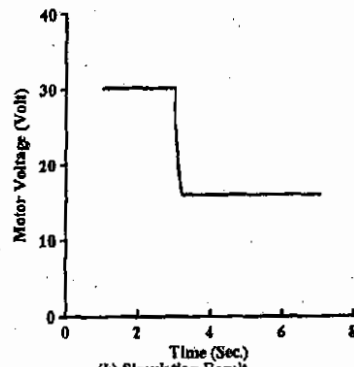


Figure (15) Source Voltage Versus Time due to Starting Condition

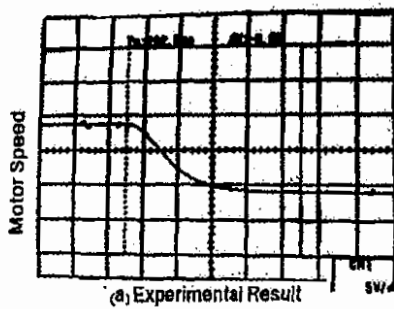




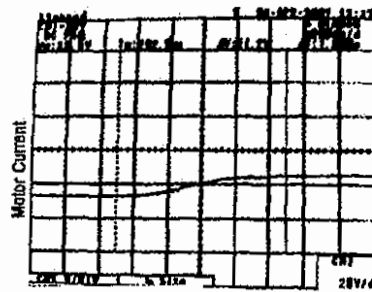
(b) Simulation Result
Figure (16) Motor Speed Versus Time Due to A Positive Step Change in The Control Voltage



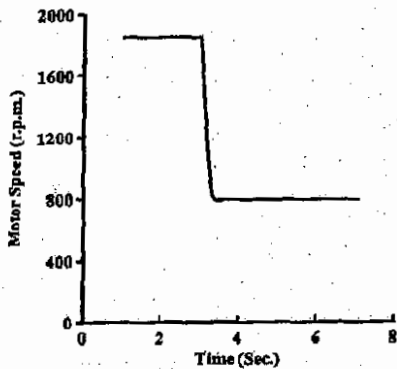
(b) Simulation Result
Figure (18) Motor Voltage Versus Time Due to A Negative Step Change in The Control Voltage



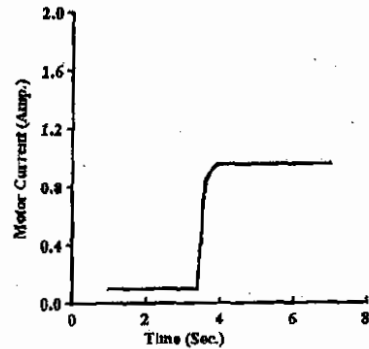
(a) Experimental Result



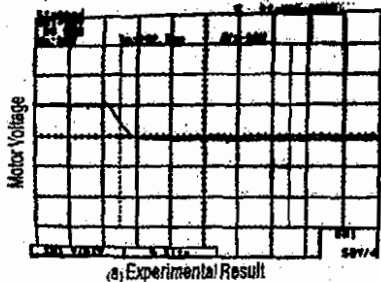
(a) Experimental Result



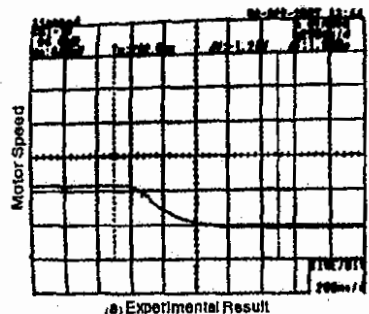
(b) Simulation Result
Figure (17) Motor Speed versus Time Due to A Negative Step Change in The Control Voltage



(b) Simulation Result
Figure (19) Motor Current Versus Time Due to Positive Change in Load



(a) Experimental Result



(a) Experimental Result

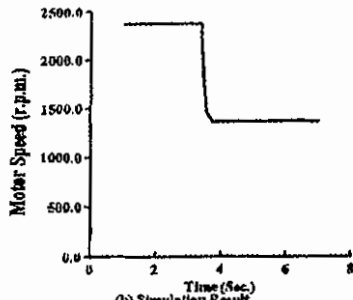
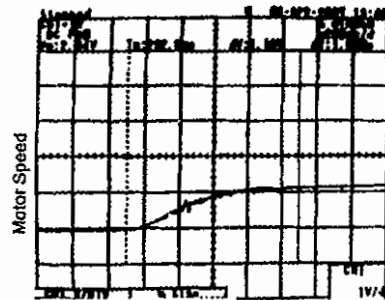
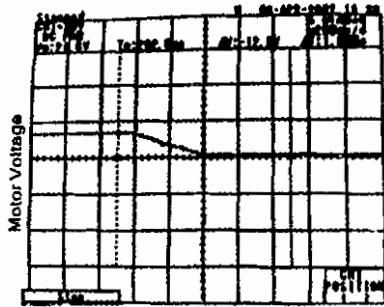


Figure (20) Motor Speed Versus Time Due to Positive Change in Load



(a) Experimental Result



(a) Experimental Result

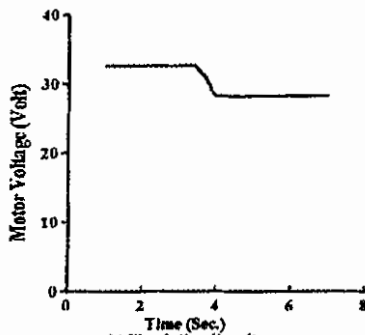


Figure (21) Motor Voltage Versus Time Due to Positive Change in Load

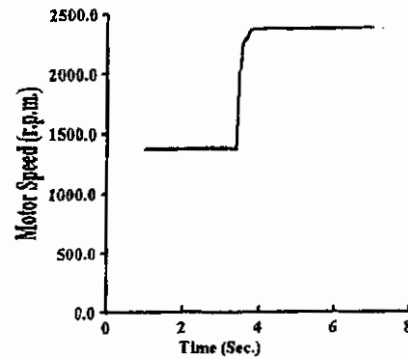
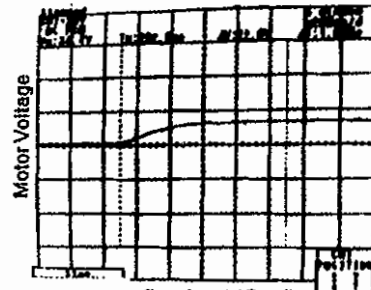
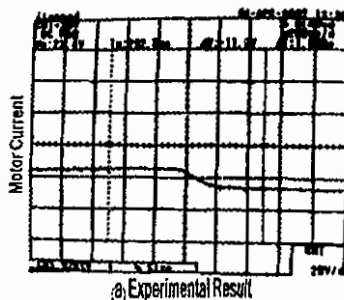


Figure (23) Motor Speed Versus Time Due to Negative Change in Load



(a) Experimental Result



(a) Experimental Result

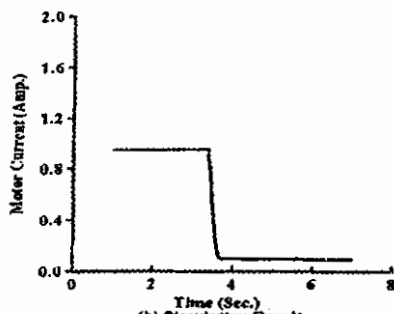


Figure (22) Motor Current Versus Time Due to Negative Change in Load

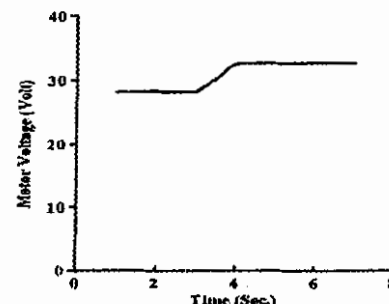


Figure (24) Motor Voltage versus Time Due to Negative Change in Load

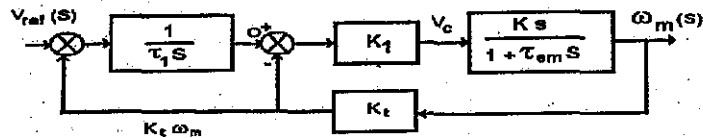


Figure (25) Complete Block Diagram for Closed Loop System

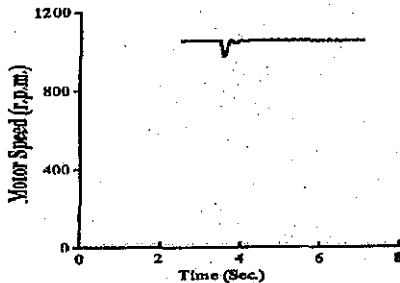
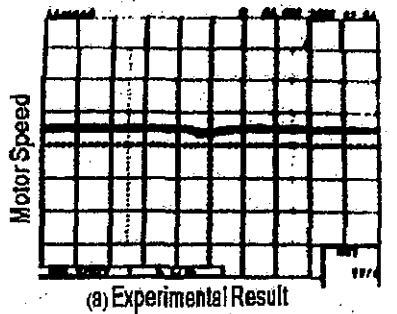


Figure (26) Motor Speed Versus Time Due to A Positive Load Change During The Closed Loop Operation

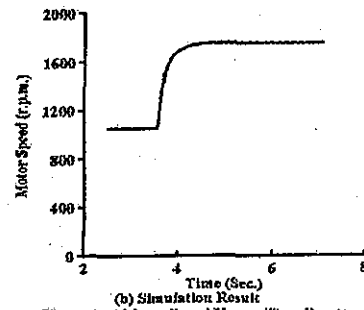
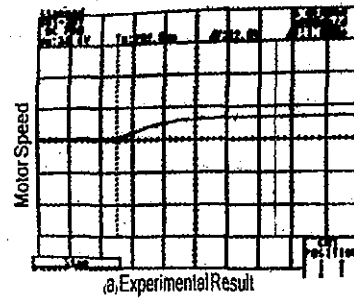


Figure (27) Motor Speed Versus Time Due to A Positive Reference Change During The Closed Loop Operation

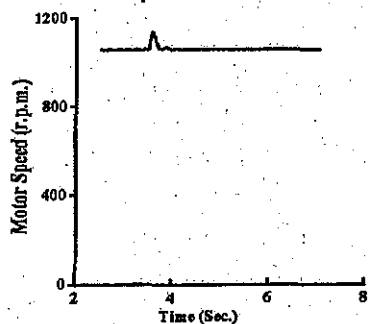
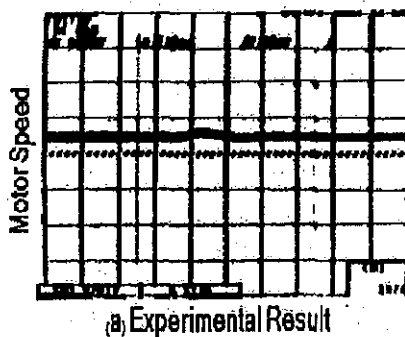


Figure (28) Motor Speed Versus Time Due to A Negative Load Change During The Closed Loop Operation

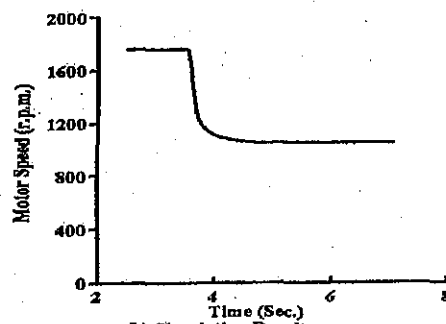
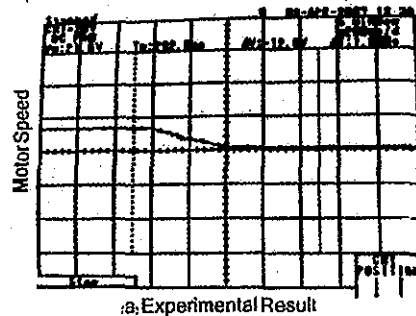


Figure (29) Motor Speed Versus Time Due to A Negative Reference Change During The Closed Loop Operation